

Research Article

An Improved Method for Estimating the Domain of Attraction of Passive Biped Walker

Yu Wang , Heng Cao, and JinLin Jiang

School of Mechanical and Power Engineering, East China University of Science and Technology, Shanghai 200237, China

Correspondence should be addressed to Yu Wang; kingem@126.com

Received 22 January 2019; Accepted 21 March 2019; Published 7 April 2019

Academic Editor: Charalampos Skokos

Copyright © 2019 Yu Wang et al. This is an open access article distributed under the Creative Commons Attribution License, which permits unrestricted use, distribution, and reproduction in any medium, provided the original work is properly cited.

An indicator of a passive biped walker's global stability is its domain of attraction, which is usually estimated by the simple cell mapping method. It needs to calculate a large number of cells' Poincare mapping result in the estimating process. However, the Poincare mapping is usually computationally expensive and time-consuming due to the complex dynamical equation of the passive biped walker. How to estimate the domain of attraction efficiently and reliably is a problem to be solved. Based on the simple cell mapping method, an improved method is proposed to solve it. The proposed method uses the multiple iteration algorithm to calculate a stable domain of attraction and effectively decreases the total number of Poincare mappings. Through the simulation of the simplest passive biped walker, the improved method can obtain the same domain of attraction as that calculated using the simple cell mapping method and reduce calculation time significantly. Furthermore, this improved method not only proposes a way of rapid estimating the domain of attraction, but also provides a feasible tool for selecting the domain of interest and its discretization level.

1. Introduction

Due to the energy-efficient of passive dynamic walking, the study of the passive biped walker is a popular area of scientific research [1, 2]. These passive biped walkers can walk stably on a downhill slope only in the interaction between the leg and environment. The stable gait is usually a periodic or cyclic gait, which is shown as a manifold in the state space or a limit cycle in the two-dimension phase diagram [3]. However, these passive biped walkers will lose their stability when they are moving from a wrong initial state or encountering a very small disturbance [4]. An indicator of a passive biped walker's global stability is its Domain Of Attraction (DOA), which is a set of all appropriate initial states that lead the walker to the perpetual walking. The walker with a larger DOA can walk stably in more complex walking conditions and increase tolerance to more disturbances in the uncertain environments. The DOA of the passive biped walker can be enlarged by actuating some joints with a control algorithm [5]. It is an important way to evaluate the performance of different control algorithms by comparing the sizes of their DOAs. Besides, the DOA can effectively guide to build some

robust prototypes [6, 7]. The detailed structure of DOA is an important aspect of studying the nonlinear properties of the passive biped walker [8, 9].

The Simple Cell Mapping (SCM) method is usually used to estimate the DOAs of different passive biped walkers [6, 7, 10]. The SCM method is an effective way to study the global stability of nonlinear dynamical systems, and its basic idea is to obtain the global properties of system by using the ordered information of local finite cells rather than investigating the properties of all states in the infinite state space [11–13]. However, there are still some issues to be solved when estimating the DOA of passive biped walker by the SCM method.

For making some concepts clearly, the basic procedures of the SCM method are introduced as follows [11, 13]. Firstly, a feasible continuous domain with boundary is chosen from the infinite state space as the Domain Of Interest (DOI). The state space outside of the DOI is sink zone. Secondly, the DOI is discretized into a large number of (P) small uniform cells which are called regular cells. These regular cells are sequentially numbered with positive integers 1 to P . The sink zone is regarded as the sink cell and numbered as 0. Thirdly,

these numbered regular cells are classified to different groups by the classification algorithm. The cells in the same group have similar global properties. Suppose that the dynamics of an entire regular cell are represented by the dynamics of its central point. By taking the central point of a regular cell numbered k as the initial condition of the Poincare mapping R , the cell that contains its image point is called the image cell of regular cell k . The mapping procedure $k \rightarrow R(k)$ is called cell-to-cell mapping or cell mapping procedure. Specially, the image cell of the sink cell is itself since the system's evolution outside the DOI is out of our interest. At the same time, if the evolution of a cell cannot reach the Poincare section in a limited time, the image cell of this cell is appointed to the sink cell. The classification algorithm of these regular cells is to generate many mapping sequences based on the relationship of the regular cells and their image cells. A typical mapping sequence starts with an unclassified cell and continuously increases by adding the image cell of the sequence's last cell to the sequence, like $k \rightarrow R(k) \rightarrow R(R(k)) \rightarrow R^3(k) \rightarrow \dots$. The mapping sequence will stop when the image cell is a sink cell or a repetitive cell in the mapping sequence. According to the classified state of the end cell, the cells in the mapping sequence are classified to different groups. If the mapping sequence ends in the sink cell, all cells in the mapping sequence are classified to the sink group. If the end cell is unclassified, all cells in the mapping sequence are classified to a new group. If the mapping sequence is encountered with an already classified cell, all cells in the mapping sequence are classified to the exist group which contains the already classified cell. The mapping sequence will be generated repeatedly until all regular cells are classified. Each group contains some attractor cells and their basins of attraction. The DOA consists of all groups except the sink group.

There are three problems to be solved when using the SCM method to estimate the DOA of a passive biped walker. Firstly, there are no clear criteria to select a feasible DOI especially for the system without any prior knowledge. Because the DOI limits the scope of the feasible states and determines the evaluation result of a regular cell, it is important to select a proper DOI. Secondly, it is also uncertain to determine the discretization level of DOI. On the one hand, the DOI should be discretized at a high discretization level to satisfy the accuracy requirement. On the other hand, the Poincare mapping is usually computationally expensive and time-consuming due to the complex dynamical equation of a passive biped walker. The discretization level cannot be too high for avoiding the memory space and computation time out of tolerance. So, the discretization level of DOI is a key factor that affects the accuracy of results and the efficiency of estimating method. Thirdly, the memory space is limited in the cell classification procedure. It needs a lot of memory space to store the classified state of each regular cell based on the cell classification algorithm. This will make the memory space is insufficient when the number of regular cells is large.

Some researchers have tried different ways to solve these problems. Jeon et al. selected the DOI of the simplest biped walker by calculating its theoretical falling boundary [14], but this method was difficult to apply for those complicated

biped walkers which had complex falling boundaries. Zhang et al. proposed a bisection method to quickly determine the approximate edge of the simplest passive biped walker's DOA, but this method must know the fixed point at the beginning and the obtained edge was too rough [15]. For avoiding the problem caused by a large amount of computation, the direct way is to increase the speed of calculating a single cell's Poincare mapping. Li et al. proposed an algorithm to accelerate the speed of Poincare mapping in the heterogeneous platforms with CPU and GPU, but it is only used in some simpler walkers due to the programming method [9]. Another feasible way is to minimize the number of Poincare mappings while meeting the same accurate requirement. Liu et al. presented the Poincare-like-alter-cell-to-cell mapping method to decrease the total number of Poincare mappings [16].

This paper proposes a method to improve the SCM method for dealing with the aforementioned problems. The proposed method uses the multiple iteration algorithm to gradually increase the discretization level of DOI for decreasing the total number of Poincare mappings and uses the domain stability as the stopping criterion of iterations for ensuring the result is accuracy. The improved method mainly contains two stages, i.e., the cell deletion procedure and the cell refinement procedure. The cell deletion procedure finds and removes a stable failure domain from DOI, and the cell refinement procedure finds a stable DOA from the remaining domains of DOI. For finding a stable domain, the change rate of domain's volume at different discretization levels, which are generated by decreasing the size of cell in each iteration, is taken as the indicator of domain stability. The DOI can be selected by repeatedly removing a stable failure domain from an uncertain wide state space until the scope of valid domain is stable. The discretization level of DOI can be determined when the stable DOA is found. Since the cells in the failure domain have been removed before cell classification, the shortage problem of memory space is also solved. At last, the proposed method improves the overall efficiency of estimating process by reducing the total number of cell mappings without losing the accuracy of results.

In the cell mapping method, a common and popular tool named the subdivision algorithm also uses the iterative method to improve the accuracy of solutions. Dellnitz et al. introduced the subdivision algorithm for obtaining the invariant sets of nonlinear dynamical systems [17]. This algorithm can be integrated with most cell mapping methods to solve different problems, such as the multiobjective optimization problems [18] and the high-dimensional problems [13]. Although both the subdivision algorithm and the proposed method in this paper use the iterative method to decrease the number of cell mappings, they have different goals. The subdivision algorithm focuses on finding the invariant sets and the attractor cells with high accuracy and efficiency. However, the proposed method in this paper uses the iterative method to generate the domains at different discretization levels for verifying the stability of domain.

The rest of the paper is organized as follows. The basic ideas and detailed procedures of the proposed method are introduced in Section 2. In Section 3, the proposed method is

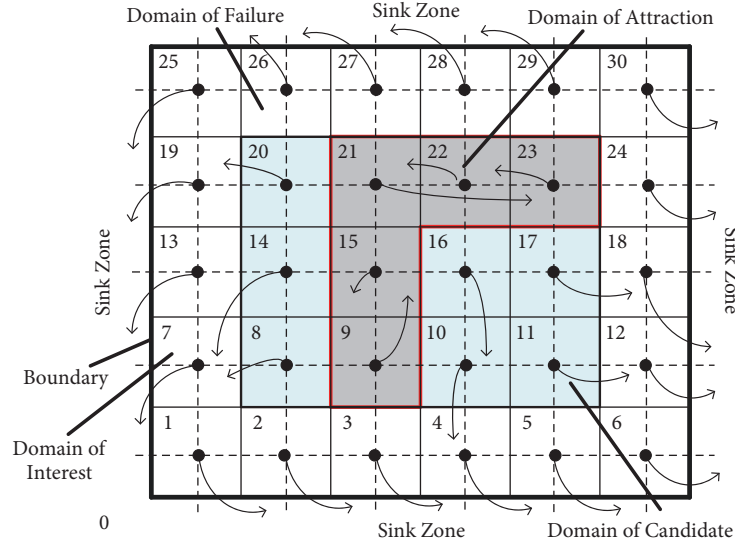


FIGURE 1: The domains in a two-dimensional system.

applied on estimating the DOA of the simplest passive biped walker. To further improve the performance of the proposed method, some key issues are discussed in Section 4. Section 5 provides some conclusions about this paper.

2. Method

2.1. Introduction of Method. In the SCM method, the whole state space is divided into the DOI and the sink zone by the boundary of DOI. By discretizing the DOI, many regular cells are generated and taken as the initial conditions of Poincare mappings. According to the location of respective image cell, the regular cells can be classified into two classes. If the image cell of a regular cell is outside the DOI, the regular cell will lose opportunity to become the member cell of DOA. This regular cell is defined as failure cell. If the image cell of a regular cell is inside the DOI, the regular cell still has opportunity to become the member cell of DOA. This regular cell is defined as candidate cell. The domain covered by all failure cells is called Domain Of Failure (DOF) and the domain covered by all candidate cells is called Domain Of Candidate (DOC). Obviously, the DOI consists of the DOF and the DOC. Under different discretization levels, the DOI has its corresponding DOF and DOC.

Figure 1 illustrates the domains of state space in a two-dimensional system. The state space consists of the DOI and sink zone. The DOI contains a group of cells numbered from 1 to 30. The Poincare mapping is denoted as the arrow line, which points to the image point from the central point of a regular cell. The white cells are mapped into the sink zone, so they are the member cells of the DOF. The blue and grey cells are the member cells of the DOC, because their image cells are still inside the DOI. Especially, the grey cells are the member cells of the DOA since they have periodic relationship with each other.

The DOA of the passive biped walker is usually small, which means a lot of regular cells are finally mapped into the sink zone. Since it only takes one step for the failure cell to map into the sink zone, we can find and delete the DOF which contains all failure cells from the whole DOI before cell classification. This will reduce the number of cells whose classified states need to be stored in cell classification. In order to find these failure cells, the image cell of each regular cell should be firstly obtained. Considering that the Poincare mapping result of a cell is totally independent of other cells, the image cells of all regular cells can be obtained together by any practicable parallel algorithm to improve the computing efficiency. Because these failure cells are no longer involved in cell classification, they have no effect on estimating the DOA. Therefore, the DOF can be found and deleted from the DOI at a lower discretization level for decreasing the total number of Poincare mappings. To compensate for the accuracy loss caused by a low discretization level, the DOA will be obtained from the remaining domains at a higher discretization level. From a low discretization level to a high discretization level, the whole method is divided into two procedures. The former is called cell deletion procedure, and the latter is called cell refinement procedure. How to determine two different discretization levels is a main challenge. The stability of domain is introduced to solve it. If the volume of a domain changes very little with discretization level increasing, the domain can be considered stable. The volume of a domain is equal to the number of contained cells multiplied by the volume of one cell. When a domain just enters the stable state, the discretization level is the optimal value. To verify the stability of a domain, the DOI should be discretized twice at two different discretization levels and the image cells of all regular cells also should be obtained twice. If this approach is applied, the total number of Poincare mappings will increase rather than decrease. We noted that the regular cell has a boundary like the DOI, so the cell also can be

discretized into many smaller cells as the discretization of DOI. If these discrete smaller cells exactly have the same central points as the regular cells which are generated by discretizing the DOI at a higher discretization level, the effect of cell discretization is equal to discretizing whole DOI from a low discretization level to higher. Then, the cell discretization technique can be used to verify the stability of domain. Through discretizing all cells in a domain, the discrete smaller cells will form a new domain after deleting the cells that no longer belong to the domain. By comparing two volumes of the domain before and after cell discretization, a change rate of domain's volume is obtained. The iteration algorithm is used to judge the criterion of domain stability for avoiding repeated calculation. In our improved method, it needs to verify the stability of DOF in cell deletion procedure and the stability of DOA in cell refinement procedure respectively. Through all iterations in two procedures, the discretization level of DOI will gradually increase with the number of iterations. When the iteration stops, the obtained DOA is stable and the discretization level of DOI is confirmed.

Based on above ideas, the implementation steps of improved method are presented in the following.

Step 1 (set some simulation parameters). The scope of the DOI Ω and the initial discretization level P_0 are the basic parameters in the initial discretization of DOI. The deletion accuracy ξ and the maximum deletion iteration number Nk are the termination parameters of the cell deletion procedure. The refinement accuracy ε and maximum refinement iteration number Nr are the termination parameters of the cell refinement procedure. The cell discretization level L is the required parameter for cell discretization.

Step 2 (get a stable DOF by cell deletion procedure). The DOI is discretized with the initial discretization level P_0 . After getting the image cells of all regular cells by Poincare mapping, the initial DOF F_0 consists of all failure cells and its volume is U_0 . For ensuring the DOF is stable, the change rate of the DOF's volume should satisfy the deletion accuracy ξ . In the k -th iteration, all cells of DOF F_{k-1} are discretized into smaller cells with cell discretization level L and a new DOF F_k consists of these failure cells in discrete cells. At this time, the corresponding discretization level of DOI is P_k . The iteration will stop until $|U_k/U_{k-1} - 1| \leq \xi$, where U_{k-1} and U_k are the volume of DOF F_{k-1} and DOF F_k respectively. The iteration also stops when the number of iterations exceeds the maximum deletion iteration number Nk . When the iteration stops, a stable DOF is obtained. After deleting all cells in the stable DOF from all cells in the DOI, the remaining cells form the approximate DOC.

Step 3 (get a stable DOA by cell refinement procedure). After a cell classification procedure, all failure cells in the approximate DOC are further deleted and the initial DOC C_0 consists of the remaining cells. The initial DOA A_0 is also obtained and its volume is V_0 . For ensuring the DOA is stable, the change rate of the DOA's volume should satisfy the refinement accuracy ε . In the r -th iteration, all cells of DOC C_{r-1} are discretized into smaller cells with cell discretization

level L and a new DOC C_r consists of these candidate cells in discrete cells. At this time, the corresponding discretization level of DOI is P_r . A new DOA A_r is obtained from the cells in new DOC C_r by the cell classification. Suppose that V_{r-1} and V_r are the volume of DOA A_{r-1} and DOA A_r respectively, the iteration stops when $|V_r/V_{r-1} - 1| \leq \varepsilon$. The iteration also stops when the number of iterations exceeds the maximum refinement iteration number Nr . When the iteration stops, the stable DOA is obtained and the final discretization level of DOI is confirmed.

Because there are many iterations to verify the stability of domain in two procedures, this improved method could be called Multiple Iterations Cell Mapping (MICM) method. Figure 2 illustrates the flow chat of the MICM method.

2.2. Cell Discretization. The cell discretization is the key technique of the MICM method, so its detailed algorithm is introduced in this section. For avoiding confusion, the cells at different discretization levels must have a unified representation method before and after cell discretization, so the cell index and cell vector are introduced firstly.

For a N -dimensional system, if the coordinate axis of a state variable x_i is divided into a large number (P_i) of intervals with an interval size h_i , the interval z_i along the x_i -axis is defined as the one which contains all x_i satisfying

$$(z_i - 0.5)h_i \leq x_i \leq (z_i + 0.5)h_i \quad i = 1, 2, \dots, N \quad (1)$$

where z_i is an integer.

Obviously, the central point of the interval is $x_i^d = z_i h_i$. At this time, the DOI is discretized into $P = P_1 \times P_2 \times \dots \times P_N$ rectangular cells with the cell size $H = [h_1, h_2, \dots, h_N]$, and the volume of one cell is $V = h_1 \times h_2 \times \dots \times h_N$.

From (1), an arbitrary state variable x_i will stay in the z_i interval, where

$$z_i = \text{Int} \left(\frac{x_i}{h_i} + 0.5 \right) \quad i = 1, 2, \dots, N \quad (2)$$

and $\text{Int}(y)$ denotes the largest integer which is less than or equal to y .

Then, an arbitrary point $X = [x_1, x_2, \dots, x_N]$ is located in the cell $Z = [z_1, z_2, \dots, z_N]$, and Z is the cell vector of this cell. The central point of cell Z is $X^d = [x_1^d, x_2^d, \dots, x_N^d] = [z_1 h_1, z_2 h_2, \dots, z_N h_N]$.

Before cell classification, all regular cells should be numbered sequentially to a positive integer sequence. The number of a cell is called cell index. There is a one-to-one consistent match between each cell index and each cell vector. Specially, if anyone component of a cell vector is out of the boundary of DOI, this cell is the sink cell and its cell index is appointed to 0.

Suppose that the first cell vector in DOI is $Z^1 = [z_1^1, z_2^1, \dots, z_N^1]$, which can be obtained by the low boundary of DOI with (2). Then, the cell index of $Z = [z_1, z_2, \dots, z_N]$ can be generated by

$$n = u(z_1 - z_1^1, z_2 - z_2^1, \dots, z_N - z_N^1) \quad n = 1, 2, \dots, P \quad (3)$$

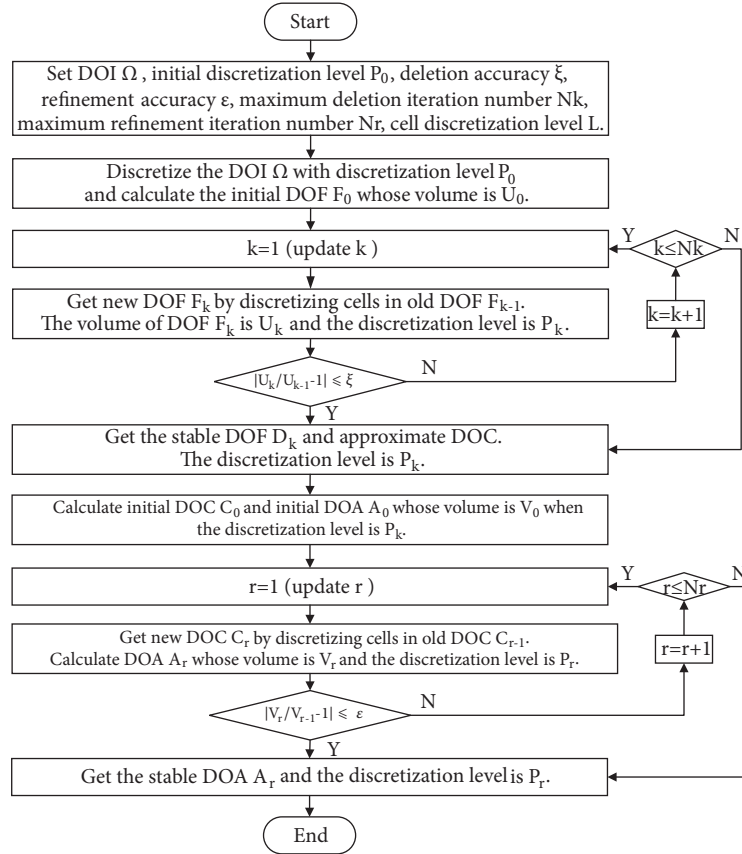


FIGURE 2: Flowchart of the MICM method.

where u is an invertible function. The cell vector of the cell index n can be obtained by

$$z_i = u_i^{-1}(n) + z_i^1 \quad n = 1, 2, \dots, P \quad i = 1, 2, \dots, N \quad (4)$$

In Matlab, the corresponding cell index of a cell vector can be generated by sub2ind function, and the corresponding cell vector of a cell index can be calculated by ind2sub function.

Now, there are three attributes to describe a regular cell, e.g., the cell index n , the cell vector Z , and the central point vector X^d . If one of them is given, the another two are easily obtained.

Because the regular cell can be represented by the cell vector, the cell discretization is simplified to a process of obtaining cell vectors of all discrete cells at a high discretization level from the cell vector of a cell at a low discretization level.

Suppose that the edge z_i of the regular cell $Z = [z_1, z_2, \dots, z_N]$ along the x_i -axis is divided into p_i segments again, then the new interval size changes to $h'_i = h_i/p_i$, and the central point x_{ij}^d of the j -th segment in the edge z_i is described as

$$x_{ij}^d = x_i^d + \left(j - \frac{p_i + 1}{2}\right) h'_i = z_i p_i h'_i + \left(j - \frac{p_i + 1}{2}\right) h'_i \quad (5)$$

$$j = 1, 2, \dots, p_i \quad i = 1, 2, \dots, N$$

Considering $x_{ij}^d = z_{ij} h'_i$, the new interval z_{ij} of the corresponding j -th segment in the edge z_i can be obtained by

$$z_{ij} = z_i p_i + j - \frac{p_i + 1}{2} \quad j = 1, 2, \dots, p_i \quad i = 1, 2, \dots, N \quad (6)$$

If a regular cell Z is discretized into $p = p_1 \times p_2 \times \dots \times p_N$ rectangular cells, the cell vectors of these new cells can be obtained by (6). It is noted that p_i must be an odd number, since z_i , z_{ij} and j are all integers.

3. Case Study

3.1. Model. In following sections, the Simplest Passive Biped Walker (SPBW) is taken as an example to demonstrate the MICM method. The structure and basic motion of SPBW are shown in Figure 3. The walker has two rigid legs connected by a frictionless hinge at the hip. The hip mass M is much larger than the leg mass m . The walking cycle consists of the swing phase shown in Figure 3(a) and the collision event shown in Figure 3(b). When the walker is walking on a rigid slope, its motion is the same as a simple double pendulum. When the swing leg is moving downward to strike the ground, the role of two legs switches. That is, the swing leg becomes the stance one and vice versa. The collision takes place instantaneously and inelastic without sliding between the swing leg and the ground. In order to avoid the scuffing problem, the swing

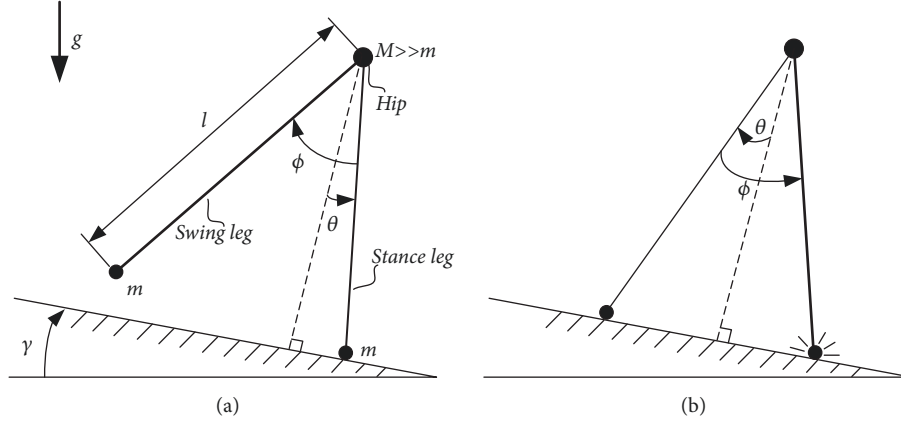


FIGURE 3: The simplest passive biped walker is walking on a slope. (a) The swing phase; (b) the collision event.

TABLE 1: Simulation parameters of the MICM method.

Parameter	Symbol	Value
Slope angle	γ	0.004
Scope of the DOI	Ω	$\theta \in [0.027, 0.876]$ $\theta + \dot{\theta} \in [-0.037, 0.029]$
Initial discretization level of the DOI	P_0	6×6
Deletion accuracy	ξ	0.2
Maximum deletion iteration number	Nk	5
Refinement accuracy	ε	0.02
Maximum refinement iteration number	Nr	5
Discretization level of each cell discretization	L	3×3

leg should be in front of the stance leg when it touches the ground. The detailed analyses of the SPBW are shown in [4].

The slope angle γ is the only variable physical parameter of SPBW. $\theta, \dot{\theta}$ are the angle and angle velocity between the stance leg and the perpendicular line of slope, respectively. $\phi, \dot{\phi}$ are the relative angle and angle velocity between the swing leg and the stance leg, respectively. The instance just after collision is set to be the Poincare section. Suppose that $q = [\theta, \phi, \dot{\theta}, \dot{\phi}]^T$ is the global state variable, then the dynamical equation of SPBW is described by

$$\begin{aligned}
 \dot{q} = & [\dot{\theta}, \dot{\phi}, \sin(\theta - \gamma), \sin(\phi)] [\dot{\theta}^2 - \cos(\theta - \gamma)] \\
 & + \sin(\theta - \gamma)]^T \quad q \notin S \\
 q^+ = & [-\theta, -2\theta, \cos(2\theta)\dot{\theta}, (1 - \cos(2\theta))\cos(2\theta)\dot{\theta}]^T \\
 & q \in S
 \end{aligned} \tag{7}$$

where S is the condition of collision and $S = \{q \mid \phi - 2\theta = 0, \dot{\phi} - 2\dot{\theta} = 0, \theta < 0\}$. If a walker can reach S in limited time from a start state, the initial state of next step q^+ is the result of Poincare mapping. Otherwise, the walker cannot walk a whole step and the result of Poincare mapping could be appointed to a state in the sink zone.

Obviously, the initial state of next step q^+ is only related to θ and $\dot{\theta}$, so $[\theta, \dot{\theta}]^T$ is fit for the independent global state variables. If so, the DOA is too tiny to distinguish its structure in the phase diagram. In order to make the DOA larger and clearer, we replace $\dot{\theta}$ with $\theta + \dot{\theta}$, which is called the pseudo angle velocity of the stance leg. Therefore, $[\theta, \theta + \dot{\theta}]^T$ is taken as the independent global state variables.

3.2. Results. The simulation parameters of the MICM method are listed in Table 1. The selection of DOI will be introduced in Section 4.1. The discretization level of cell discretization L could be any combination of odd integers, but it is uniformly set to 3×3 for simplicity in this simulation.

Figure 4 shows the processes of estimating the DOA of SPBW by the MICM method. Each regular cell is denoted as a rectangle with its central point in all figures of this paper. The failure cell, candidate cell, attraction cell have blue, green and red central point respectively. For showing the boundaries of DOF and DOC clearly, the candidate cells are not shown in cell deletion procedure and the failure cells are not shown in cell refinement procedure.

As shown in Figure 4(a), the DOI is discretized into regular cells with the initial discretization level P_0 firstly. In Figure 4(b), the initial DOF consists of the failure cells after calculating the image cells of all regular cells. Next, the cells in the initial DOF are discretized into smaller cells with

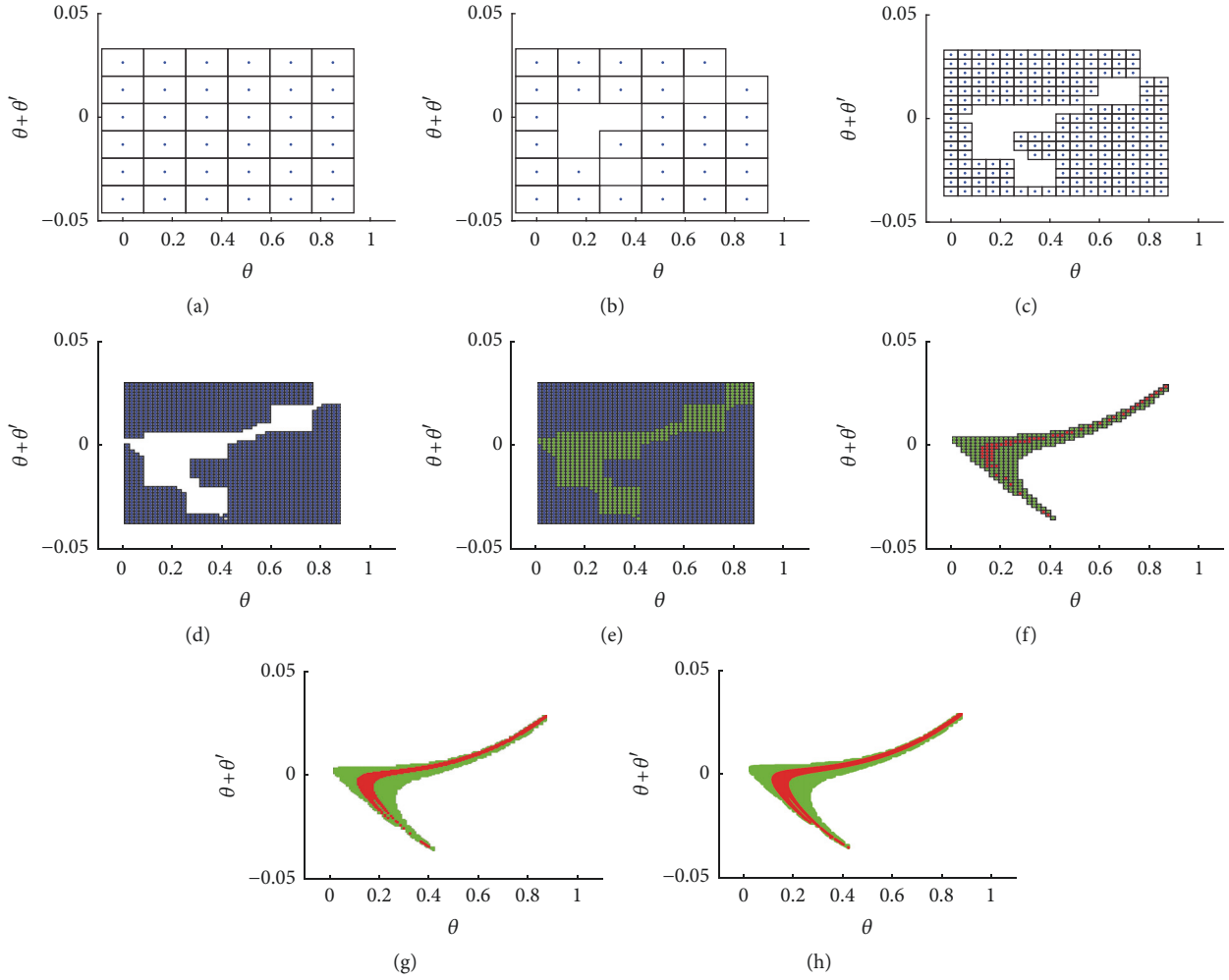


FIGURE 4: The processes of estimating the DOA of SPBW by the MICM method. (a) Initial discretization of DOI; (b) initial DOF; (c) DOF after the first iteration of the cell delete procedure; (d) stable DOF; (e) approximate DOC and stable DOF; (f) initial DOA and initial DOC; (g) DOA and DOC after the first iteration of the cell refinement procedure; (h) stable DOA and its corresponding DOC.

discretization level L , and a new DOF shown in Figure 4(c) consists of the failure cells in these smaller cells. Comparing between the initial DOF and new DOF, the change rate of DOF's volume does not satisfy the requirement of deletion accuracy ξ , so the cells in new DOF need to be discretized. After discretizing the cells in new DOF again, a newer DOF shown in Figure 4(d) is obtained. Now, the change rate of DOF's volume is lower than the deletion accuracy ξ , so the iteration stops and the stable DOF is confirmed. As shown in Figure 4(e), the approximate DOC naturally consists of these regular cells which are not in the stable DOF. Then, the cell refinement procedure starts. After a cell classification procedure, all failure cells in the approximate DOC are further deleted and the initial DOC shown in Figure 4(f) consists of the remaining cells, which the initial DOA is obtained from. As shown in Figure 4(g), the cells in the initial DOC are discretized into smaller cells with discretization level L , and a new DOC consists of the candidate cells in these smaller cells. After that, the new DOA is obtained by cell classification. Since the change rate of DOA's volume does not

satisfy the refinement accuracy ε , the cells in the new DOC have to be discretized again. A newer DOC and DOA shown in Figure 4(h) is obtained after a cell classification procedure. At this time, the change rate of DOA's volume is lower than the refinement accuracy ε , so the iteration stops and the stable DOA is obtained.

Figure 5 shows the growing trend of the number of mappings and the volume of domain with the iteration. In both procedures, the number of mappings increases from a low number with the iteration increasing. Especially in the cell refinement procedure, the number of mappings, which is the maximum number of cells to be stored in cell classification, is far less than the number of mappings in SCM method. It means that the MICM method can effectively reduce the requirement of memory space in cell classification procedure.

After above processes, the DOI is finally discretized into 406×406 cells. Through 26267 Poincare mappings and 2 cell classification procedures, the DOA of SPBW contains 5127 cells. Using the same parameters and discretization level in

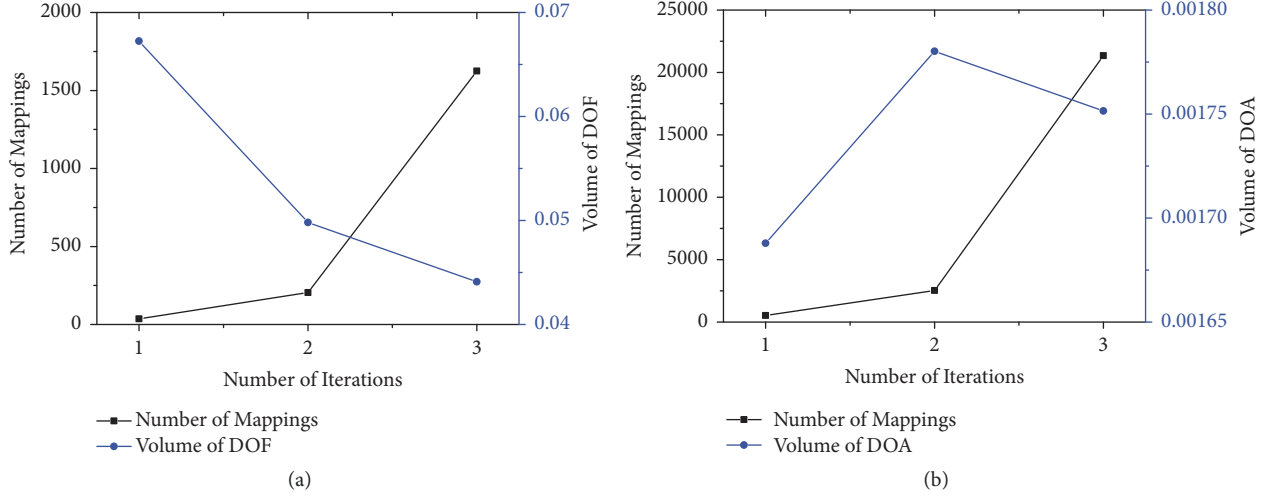


FIGURE 5: The number of mappings and the volume of domain at each iteration. (a) The curves of the cell deletion procedure; (b) the curves of the cell refinement procedure.

the SCM method, the DOA consists of 5162 cells through 164836 Poincare mappings and 1 cell classification procedure. Although 35 cells missed in the DOA obtained by the MICM method, the total number of Poincare mappings sharply decreases. Because the Poincare mapping is a consuming-time process, the MICM method saves much time. For an estimation process, it is worthy to accelerate the computation with a little accuracy loss.

4. Discussions

4.1. Selection of the Domain of Interest. If there is no prior knowledge about a system, a proper DOI should be selected before formal simulation. The selection of DOI is a procedure of removing the infeasible domains from whole state space, so the cell deletion procedure, which can efficiently remove the failure domains from a given domain, will be useful to select the DOI.

The details of selecting the DOI with the cell deletion procedure are presented as follows. Firstly, a wider initial DOI is chosen to be the basic research scope. Next, a DOC can be obtained from the DOI by using a cell deletion procedure with a lower deletion accuracy. If the scope of DOC is not closed to the scope of the DOI, the scope of DOC is used to be a new DOI for next iteration. Otherwise, the scope of DOC is taken as the formal DOI.

The selection of SPBW's DOI is taken as an example. The scope of initial angle and angular velocity of stance leg should be estimated firstly. The scope of initial angle of stance leg is easy to determine since it is only limited by the physical conditions. So the initial angle of stance leg certainly belongs to $[0, \pi/2]$. However, the scope of initial angular velocity of stance leg is hard to be estimated, because it is limited not only by the physical conditions but also by the complex dynamical equations. The initial angular velocity of stance leg is obviously negative since the stance leg must move forward,

so the scope of pseudo angle velocity can be set to $[-10, \pi/2]$. Figure 6 illustrates the processes of selecting the DOI of SPBW. The boundary of the DOI at each iteration is denoted by the blue rectangular. After five iterations, the formal DOI is obtained. As shown in Figure 6(g), the formal DOI is $\theta \in [0.027, 0.876]$ and $\theta + \dot{\theta} \in [-0.037, 0.029]$, which is used in the former simulation.

4.2. Boundary Refinement. Comparing with the DOA obtained by the SCM method, there are a few cells missed in the DOA obtained by the MICM method. The reason is that some domains are wrongly covered by the DOF when the discretization level is low. After many iterations in the cell deletion procedure, these domains cannot be covered by the approximate DOC at the discretization level of stable DOF. For decreasing the lost cells, it needs to find these wrong domains and add them into the approximate DOC at a higher discretization level. Since most lost cells are located near the boundaries of DOF and DOC, the domains that contain the cells on the stable DOF's boundary should be considered firstly. These boundary cells will be discretized into smaller cells, and the discrete cells need to be verified for finding the domains where they really belong to by Poincare mapping. Because these boundary cells are discretized again for further verification, the total number of Poincare mappings will increase. This procedure mainly focuses on the boundary cells, so it can be called boundary refinement.

Figure 7 shows the processes of estimating the DOA of SPBW by the MICM method with the boundary refinement. Because the processes of cell deletion procedure are the same as Figures 4(a)–4(d), Figure 7 only shows the processes after finding the stable DOF. As shown in Figure 7(a), the boundary cell is donated by a rectangular with yellow central point. The cell discretization level in boundary refinement is also set to $L = 3 \times 3$. In Figure 7(b), the approximate DOC at a higher discretization level is obtained after the boundary

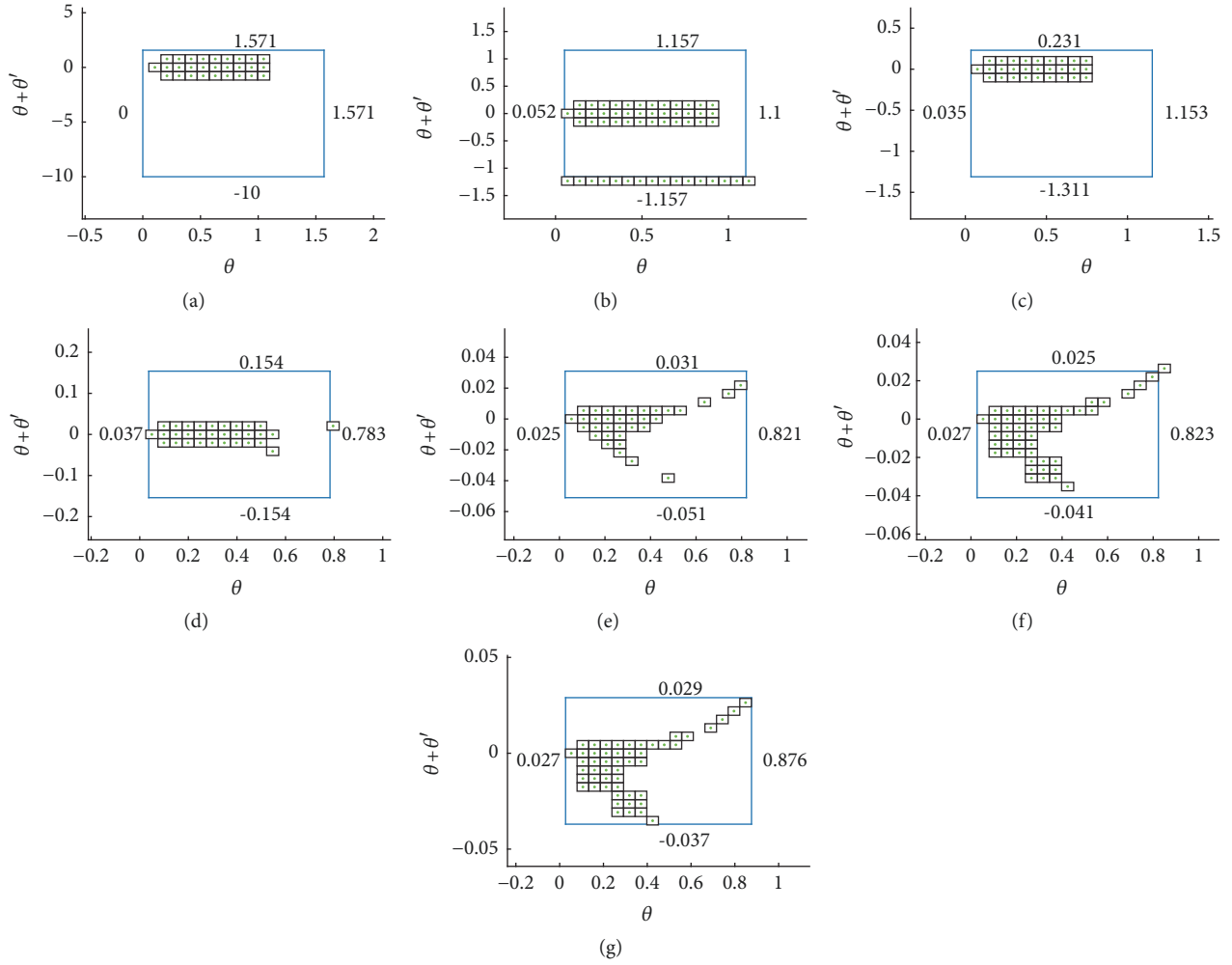


FIGURE 6: The processes of selecting the DOI of SPBW. (a) Initial DOI and DOC (b) DOI and DOC after the first iteration; (c) DOI and DOC after the second iteration; (d) DOI and DOC after the third iteration; (e) DOI and DOC after the fourth iteration; (f) DOI and DOC after the fifth iteration; (g) the formal DOI.

refinement procedure. The initial DOA and initial DOC are shown in Figure 7(c). After only one iteration, a stable DOA is obtained as shown in Figure 7(d). Comparing with the DOA obtained by the MICM method without the boundary refinement, the missing cells decreases to 6 from 35, but the total number of Poincare mappings increases to 30471 from 26267.

Table 2 shows the comparison between SCM method and MICM method for estimating the DOA of SPBW when the slope angle is 0.004 rad and the DOI is discretized into 406×406 cells. All simulations are implemented by Matlab2014b on the computer with 8G RAM and Intel® Core™ i7-6820HQ CPU. From the results, it can be seen that the accuracy of results is at the cost of time and computation. We can choose whether to add the boundary refinement procedure to the MICM method for satisfying different requirements. If the accuracy of results needs to be very high, it is better to estimate the DOA by the MICM method with boundary refinement. If it just needs to find the approximate

DOA quickly, the best way is to use the MICM method without boundary refinement.

5. Conclusions

This paper presents a new multiple iterations cell mapping method for estimating the DOA of the passive biped walker. The MICM method consists of two procedures, i.e., the cell deletion procedure and the cell refinement procedure. The cell deletion procedure not only can delete DOF from the DOI at a low discretization level, but also can select a proper DOI from an uncertain wide state space. The cell refinement procedure can quickly find a stable DOA at a high discretization level. The major improvement of the MICM method is that the DOI is selected by the cell deletion procedure instead of many trails and the discretization level of DOI is determined by the cell refinement procedure instead of prespecified artificially. Comparing

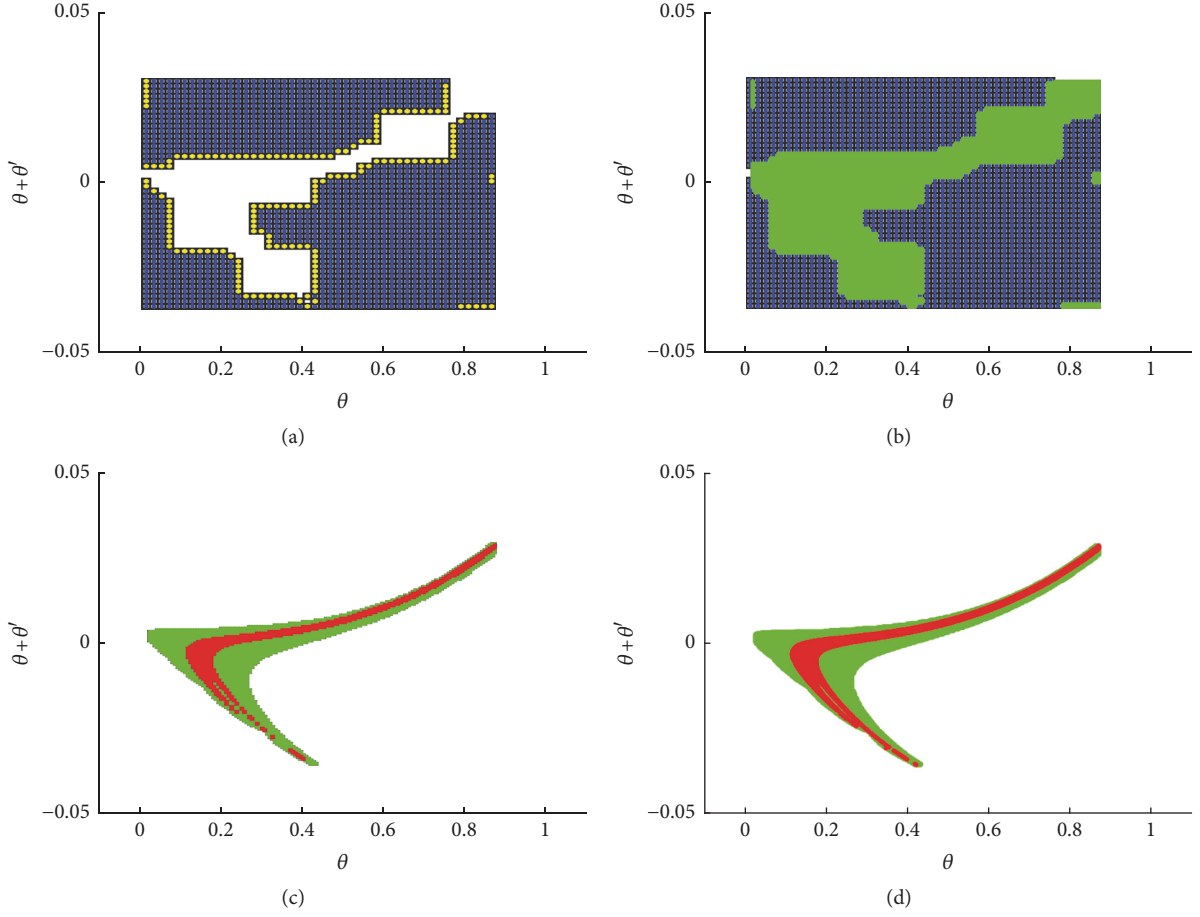


FIGURE 7: The processes of estimating the DOA of SPBW by the MICM method with boundary refinement. (a) The boundary cells in the stable DOF; (b) approximate DOC and stable DOF; (c) initial DOA and initial DOC; (d) the stable DOA and its corresponding DOC.

TABLE 2: Comparison between SCM method and MICM method for estimating the DOA of SPBW.

Method	Number of Poincare mappings	Number of cells in DOA	Percent of decreasing Poincare mappings	Percent of missing cells	Time[s]	Speed up
SCM method	164836	5162	-	-	530.72	-
MICM method without boundary refinement	26267	5127	84.06%	0.68%	89.03	5.96×
MICM method with boundary refinement	30471	5156	81.51%	0.15%	103.25	5.14×

with the results of the SCM method, the new method can obtain the same DOA with much less calculation and time.

The MICM method can ensure the DOA reliable and yet avoid excessive calculation, so it is a valuable analysis tool for the passive biped walker. Although this paper only takes the simplest passive biped walker as an example to describe the usage of the MICM method, it also can be used to estimate the DOA of more complex passive biped walkers that have more global states variables. Since the MICM method is

based on the SCM method, it can be used not only for the complex dynamical systems like the passive biped walker, but also for other nonlinear dynamical systems which have small DOAs.

Data Availability

The data used to support the findings of this study are available from the corresponding author upon request.

Conflicts of Interest

The authors declare that there are no conflicts of interest regarding the publication of this paper.

Acknowledgments

This research is supported by the National Natural Science Foundation of China [91748110].

References

- [1] S. Collins, A. Ruina, R. Tedrake, and M. Wisse, "Efficient bipedal robots based on passive-dynamic walkers," *Science*, vol. 307, no. 5712, pp. 1082–1085, 2005.
- [2] T. McGeer, "Passive dynamic walking," *International Journal of Robotics Research*, vol. 9, no. 2, pp. 62–82, 1990.
- [3] A. Goswami, B. Espiau, and A. Keramane, "Limit cycles in a passive compass gait biped and passivity-mimicking control laws," *Autonomous Robots*, vol. 4, no. 3, pp. 273–286, 1997.
- [4] M. Garcia, A. Chatterjee, A. Ruina, and M. Coleman, "The simplest walking model: Stability, complexity, and scaling," *Journal of Biomechanical Engineering*, vol. 120, no. 2, pp. 281–286, 1998.
- [5] M. Wisse, A. L. Schwab, R. Q. van der Linde, and F. C. T. van der Helm, "How to keep from falling forward: elementary swing leg action for passive dynamic walkers," *IEEE Transactions on Robotics*, vol. 21, no. 3, pp. 393–401, 2005.
- [6] Q. Wang, Y. Huang, and L. Wang, "Passive dynamic walking with flat feet and ankle compliance," *Robotica*, vol. 28, no. 3, pp. 413–425, 2010.
- [7] N. Liu, J. Li, and T. Wang, "The effects of parameter variation on the gaits of passive walking models: Simulations and experiments," *Robotica*, vol. 27, no. 4, pp. 511–528, 2009.
- [8] K. An, Z. Fang, Y. Li, and Q. Chen, "Internal features in basin of attraction of the simplest walking model," *Journal of Mechanical Science and Technology*, vol. 29, no. 11, pp. 4913–4921, 2015.
- [9] Q. Li and X.-S. Yang, "New walking dynamics in the simplest passive bipedal walking model," *Applied Mathematical Modelling: Simulation and Computation for Engineering and Environmental Systems*, vol. 36, no. 11, pp. 5262–5271, 2012.
- [10] M. Wisse, A. L. Schwab, and F. C. T. Van Der Helm, "Passive dynamic walking model with upper body," *Robotica*, vol. 22, no. 6, pp. 681–688, 2004.
- [11] C. S. Hsu, "A theory of cell-to-cell mapping dynamical systems," *Journal of Applied Mechanics*, vol. 47, no. 4, pp. 931–939, 1980.
- [12] Á. Castillo and P. J. Zufiria, "Cell mapping techniques for tuning dynamical systems," in *Global Analysis of Nonlinear Dynamics*, pp. 31–50, Springer, New York, NY, USA, 2012.
- [13] J. Q. Sun, F. R. Xiong, O. Schutze, and C. Hernández, *Cell Mapping Methods – Algorithmic Approaches and Applications*, Springer, Singapore, 2019.
- [14] Y. Jeon, Y.-S. Park, and Y. Park, "A study on stability of limit cycle walking model with feet: parameter study," *International Journal of Advanced Robotic Systems*, vol. 10, no. 1, Article ID 49, 2013.
- [15] P. Zhang, Y. Tian, and Z. Liu, "Bisection method for evaluation of domain of attraction of passive dynamic walking," in *Proceedings of the 4th International Conference on Autonomous Robots and Agents (ICARA)*, pp. 692–697, 2009.
- [16] L. Liu, Y. Tian, and X. Huang, "A method to estimate the basin of attraction of the system with impulse effects: application to the biped robots," *International Conference on Intelligent Robotics and Applications*, vol. 5314, no. 1, pp. 953–962, 2008.
- [17] M. Dellnitz and A. Hohmann, "A subdivision algorithm for the computation of unstable manifolds and global attractors," *Numerische Mathematik*, vol. 75, no. 3, pp. 293–317, 1997.
- [18] M. Dellnitz, O. Schutze, and T. Hestermeyer, "Covering pareto sets by multilevel subdivision techniques," *Journal of Optimization Theory and Applications*, vol. 124, no. 1, pp. 113–136, 2005.

